Research article

The second intracellular loop of the yeast Trk1 potassium transporter is involved in regulation of activity, and interaction with 14–3-3 proteins

Jakub Masaryk [a], Deepika Kale [a], Pavel Pohl [b,1], Francisco J. Ruiz-Castilla [c,2],
Olga Zimmermannová [a], Veronika Obšilová [b], José Ramos [c], Hana Sychrová [a,*]

[a] Institute of Physiology of the Czech Academy of Sciences, Laboratory of Membrane Transport, 14200 Prague 4, Czech Republic
[b] Institute of Physiology of the Czech Academy of Sciences, Laboratory of Structural Biology of Signaling Proteins, Division BIOCEV, 25250 Vestec, Czech Republic
[c] Department of Agricultural Chemistry, Edaphology and Microbiology, University of Córdoba, 140 71 Córdoba, Spain

ARTICLE INFO

ABSTRACT

Potassium is an essential intracellular ion, and a sufficient intracellular concentration of it is crucial for many processes; therefore it is fundamental for cells to precisely regulate K^+ uptake and efflux through the plasma membrane. The uniporter Trk1 is a key player in K^+ acquisition in yeasts. The *TRK1* gene is expressed at a low and stable level; thus the activity of the transporter needs to be regulated at a posttranslational level. *S. cerevisiae* Trk1 changes its activity and affinity for potassium ion quickly and according to both internal and external concentrations of K^+, as well as the membrane potential. The molecular basis of these changes has not been elucidated, though phosphorylation is thought to play an important role. In this study, we examined the role of the second, short, and highly conserved intracellular hydrophilic loop of Trk1 (IL2), and identified two phosphorylable residues (Ser882 and Thr900) as very important for 1) the structure of the loop and consequently for the targeting of Trk1 to the plasma membrane, and 2) the upregulation of the transporter's activity reaching maximal affinity under low external K^+ conditions. Moreover, we identified three residues (Thr155, Ser414, and Thr900) within the Trk1 protein as strong candidates for interaction with 14–3-3 regulatory proteins, and showed, in an in vitro experiment, that phosphorylated Thr900 of the IL2 indeed binds to both isoforms of yeast 14–3-3 proteins, Bmh1 and Bmh2.

1. Introduction

Potassium ion, being an indispensable intracellular ion, plays many essential roles, such as in the regulation of cell volume and internal pH, stabilization of membrane potential, balancing the negative charge of macromolecules, protein synthesis, and enzyme activation. In yeast cells, sufficient K^+ content is also a pivotal signal for cell division and a prerequisite for resistance to various stresses [1,2]. Nonetheless, excess internal K^+ is toxic, and it leads to the deacidification of yeast vacuoles, and, consequently, to a shortened

lifespan [3]. It is therefore of the highest importance for the yeast cells to regulate the import and export of potassium across the plasma membrane tightly in order to maintain its intracellular level within the optimal ranges of 200–300 mM [1]. Yeast cells employ a variety of K^+ uptake and efflux systems with distinct structures and transport mechanisms. For K^+ import, apparently, all yeast species possess a Trk1 uniporter, many also Hak1 K^+-H^+ symporters, and a few of them also Acu1 ATPases [4,5]. To export surplus K^+, yeast cells employ Ena ATPases, Nha1 cation/H^+ antiporters, and Tok1 channels [2].

Saccharomyces cerevisiae has no Hak1 and Acu1 K^+ importers; its genome only encodes two Trk proteins, Trk1 and Trk2. *TRK1* is dominant in potassium uptake, as its deletion substantially diminishes cell growth on low external K^+ [6]. The contribution of Trk2 to potassium acquisition in growing cells is only marginal, probably due to its very low expression [7], and its role is more important in stationary cells, where it is necessary for the survival of various stresses [8,9]. Deleting both *TRK* genes leads to not only the inability

* Corresponding author.
E-mail address: hana.sychrova@fgu.cas.cz (H. Sychrová).
[1] Present address: Ubiquitin Signaling Specificity Group, Max Planck Institute for Multidisciplinary Sciences, Göttingen, Gemany
[2] Present address: Department of Inorganic Chemistry and Chemical Engineering, University of Córdoba, Córdoba and Institute of Water Research, University of Granada, Granada, Spain
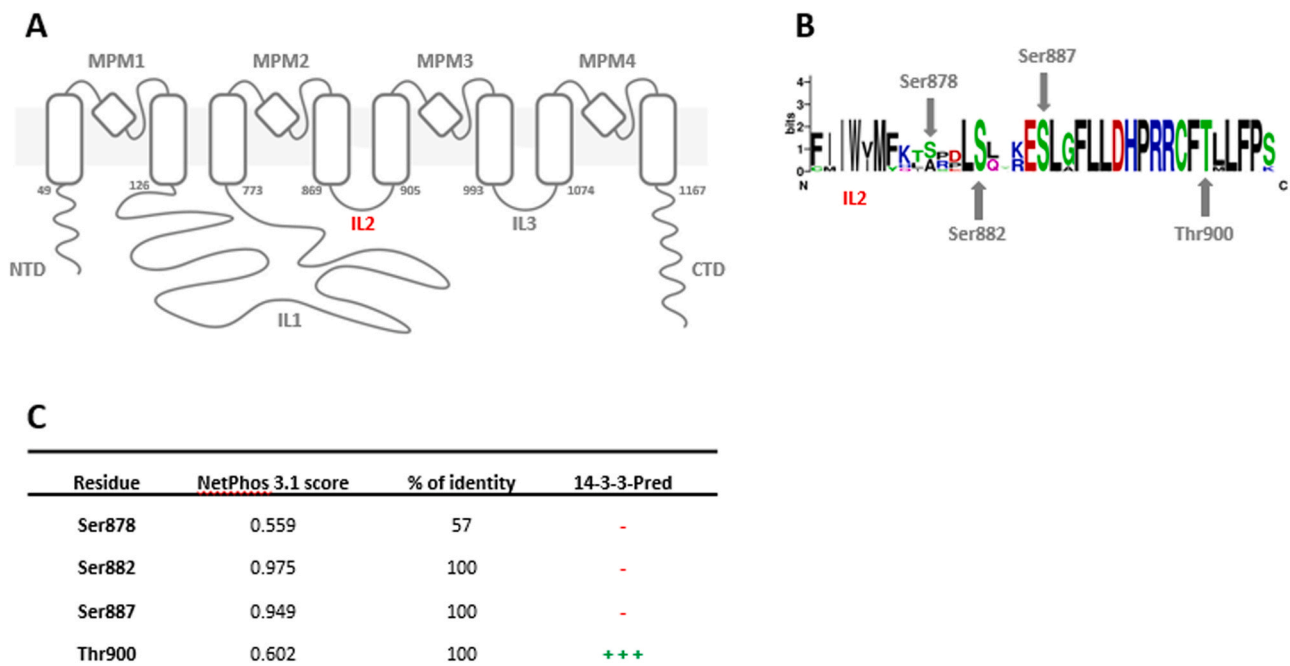
Fig. 1. Trk1 model and its intracellular loop 2. (A) Topological model of *S. cerevisiae* Trk1 with intracellular loop 2 (IL2) highlighted in red. (B) WebLogo analysis of IL2 sequences of *S. cerevisiae* Trk1 and Trk2, and Trk1s of *Candida albicans*, *C. glabrata*, *C. parapsilosis*, *C. dubiliensis*, and *Zygosaccharomyces rouxii*. Putative phosphorylation sites within IL2 of *S. cerevisiae* Trk1 are highlighted with grey arrows. (C) Potential phosphorylation sites in IL2 with their respective NetPhos 3.1 score, identity, and results of 14–3–3-Pred analysis (**+++,** residue predicted by the three algorithms as a potential 14–3–3 binding site; **-**, residue not predicted by any algorithm).

of cells to grow at low K^+ concentrations [10], but also results in the hyperpolarization of their plasma membrane and acidification of their cytosol [11].

Trk proteins of *S. cerevisiae* are integral membrane proteins with a predicted structure conserved across all yeast and fungi. According to a recent model, the *S. cerevisiae* Trk1 polypeptide chain (1235 amino acids) contains four MPM domains, each consisting of two transmembrane M-helices connected by a short pore P-helix. MPM domains are assembled around the central axis, thus creating a pore for substrate transport [12]. MPM domains are connected by intracellular and extracellular loops of various lengths. Trk1 of *S. cerevisiae* contains a very long intracellular loop connecting the first and second MPM subdomains (Fig. 1 A), whose length and sequence are not conserved among yeast Trk proteins, and which seems to not be crucial for Trk1′s transport activity [13]. Additionally, Trk1 proteins are thought to form tetramers capable of facilitating an efflux of chloride anions across the plasma membrane [14].

Besides K^+, Trk1 also transports rubidium ion, which is commonly used as a substrate to estimate Trk1′s activity and kinetic parameters [1]. Under certain conditions (a very high external concentration of Na^+ and very low external concentration of K^+), some sodium ions can enter via Trk1, but in general, the Trk1 transporter of *S. cerevisiae* is regarded as K^+-specific [1,2]. The most distinct feature of Trk1 is the ability to adjust its kinetic parameters, with affinity ranging from 180 μM to 2.5 mM, according to the availability of K^+, intracellular K^+ content, and actual membrane potential [15].

S. cerevisiae Trk1 is believed to be expressed at a constitutive and very low level, and its expression is unaffected by changes in external conditions, including changes in external K^+ concentration [1,2]. The necessary tight regulation of Trk1′s activity and affinity is therefore thought to occur at a post-translational level, mainly via phosphorylation/dephosphorylation. Various phosphoproteomic studies have led to the identification of multiple amino-acid residues as potential targets for phosphorylation (all residues identified so far are listed in Table S1). According to these studies, conditions under which Trk1 is presumably phosphorylated include the loss of one of the main N-acetyl transferases [16], exposure to the alpha factor

[17], and DNA damage [18]. Additionally, crosstalk between phosphorylation and ubiquitination was suggested to play a role in the degradation of Trk1 [19], and finally, Trk1 was indicated as a potential substrate for phosphorylation by the Cdk1 kinase [20]. Besides the global phosphoproteomic studies, several studies focusing on the involvement of specific kinases and phosphatases in the regulation of Trk1 have been performed. The kinases Hal5 [21], and Snf1 [22], as well as calcineurin phosphatase [23], stimulate the activity of Trk1. In the contrast, the phosphatases Ppz1 and Ppz2 [24] and kinase Sky1 [25] are thought to be involved in the downregulation of Trk1′s activity.

The different activity of phosphorylated/dephosphorylated transporters may fully or partially result from the binding of 14–3–3 proteins. 14–3–3 proteins are a family of small, highly conserved, regulatory proteins expressed in all eukaryotes [26]. Forming dimers, each monomer is able to bind a phosphorylated serine or threonine contained within a specific consensus sequence of binding partners [27]. The binding of 14–3–3 proteins leads to changes in the function of target proteins by various mechanisms, e.g. changes in conformation leading to either activation or inactivation [26] or the blocking of specific regulatory sequences within target proteins and thus altering their function or localization [28,29]. In *S. cerevisiae*, 14–3–3 proteins are encoded by two genes, *BMH1* and *BMH2*, with *BMH1* accounting for approximately 80% of total 14–3–3-expression [30]. Although yeast cells are able to withstand individual *BMH* deletions, suggesting an overlap in the function of the two isoforms, the combined deletion of both genes is lethal in most *S. cerevisiae* laboratory strains [31]. With up to hundreds of interaction partners [32], 14–3–3 proteins are involved in the regulation of essentially every process in yeast cells [33], and they have been shown to regulate both the subcellular localization [34] and the activity [35–37] of membrane transporters, including one of the K^+ exporters in *S. cerevisiae*, the Nha1 antiporter [35].

In order to add to existing scarce data on the regulation of Trk1, this study focuses on the identification of putative phosphorylation sites involved in the regulation of Trk1′s activity and affinity, which are mainly localized in the second short and highly conserved

intracellular loop of the protein. The involvement of a specific set of kinases and 14–3–3 proteins is also examined.

2. Materials and methods

2.1. Strains and growth conditions

Yeast strains used in this study are listed in Table S2. BYT12-derived strains with each a deletion of one of the genes encoding kinases *PTK2* (YJR059W), *SKY1* (YMR216C), *SNF1* (YDR477W), *HAL5* (YJL165C), and *HOG1* (YLR113W) were constructed by homologous recombination with a KanMX cassette and the Cre-loxP system [38] using the oligonucleotides listed in Table S3.

Yeast cultures were routinely grown in YNB (0.67% YNB (Yeast Nitrogen Base w/o Amino Acids; 291940; Difco, USA), 2% glucose, containing approx. 15 mM K^+) or YNB-F (0.17% YNB-F (Translucent K^+ free medium, Yeast nitrogen base w/o Amino Acids, Ammonium Sulphate & Potassium; CYN7502; Formedium, UK) containing approximately 15 µM K^+, 2% glucose, 0.4% ammonium sulphate; pH adjusted to 5.8 by NH_4OH) media at 30 °C. For solid media, 2% agar was added. Media were sterilised by autoclaving. A mixture of auxotrophic supplements (OMM or OMM-ura for transformed cells; [39]) was added after autoclaving.

Growth of yeast cells was compared in drop tests on solid media. Yeast cells were pre-grown on YNB plates supplemented with 100 mM KCl, collected and resuspended in sterile water to $OD_{600} \sim$ 0.6. Three additional 10-fold dilutions were prepared, and 3 µL were spotted on YNB-F plates supplemented as indicated. The pH of the plates was adjusted with either NH_4OH (pH 5.8) or diluted HCl (pH 4.0). Plates with pH 7.2 were buffered with 20 mM MOPS and NH_4OH. Plates were incubated at 30 °C. Representative results of at least three repetitions are shown.

Cells were grown in liquid YNB supplemented with 100 mM KCl for uptake measurements ($OD_{600} \sim$ 0.3–0.4) or fluorescence microscopy ($OD_{600} \sim$ 1), and they were either used directly (non-starved cells) or additionally incubated in liquid YNB-F media without added KCl for 1 h (K^+-starved cells).

2.2. Plasmids

All plasmids used in this study are listed in Table S4. A centromeric plasmid, weak and constitutive promoter and C-terminal GFP-tagging were used as this combination seemed to be optimal to observe differences brought by mutations of *TRK1* [15]. Single amino-acid substitutions were performed by site-directed mutagenesis using a QuikChange II Site-Directed Mutagenesis Kit (Agilent Technologies, Santa Clara, CA, USA) with oligonucleotides listed in Table S5. Plasmids pCScTRK1, pGRU1ScTRK1 or pCScTRK1-GFP were used as templates. All substitutions were confirmed by sequencing.

2.3. Fluorescence microscopy

To compare the localisation of Trk1 and its mutated versions, cells expressing C-terminally GFP-tagged Trk1 from either multicopy or centromeric plasmids were used. Cell images were acquired with an Olympus BX53 fluorescent microscope with an Olympus DP73 camera. A Cool LED light source (with 460 nm excitation and 515 nm emission) was used. Differential interference contrast (DIC) was used to visualise whole cells.

2.4. Uptake measurements and estimation of kinetic parameters

To estimate the activity of Trk1 and its mutated versions, Rb^+ was used as a substrate. Cells grown and starved of K^+ as described above were collected, washed with sterile water, and resuspended in MES buffer (20 mM MES, 2% glucose, 0.1 mM $MgCl_2$; pH adjusted to 5.8

with $Ca(OH)_2$) to $OD_{600} \sim$ 0.2. At time 0, RbCl was added to the desired final concentration. Five-mL samples were collected at 1-min intervals over 5 min, filtered through Millipore filters (0.8 µm pore size) and washed with 20 mM $MgCl_2$. Filters with cells were then extracted overnight in an extraction buffer (0.2 M HCl, 10 mM $MgCl_2$, 0.2% KCl). The obtained extracts were analysed by atomic absorption spectrometry, and initial rates of Rb^+ uptake in nmoles per mg dry weight of cells per minute were calculated [40]. For the estimation of kinetic parameters of Rb^+ uptake, four different concentrations of RbCl were used, ranging from 50 µM to 1 mM for K^+-starved cells and from 1 mM to 10 mM for non-starved cells. The initial uptake rates obtained for each Rb^+ concentration were plotted on a Lineweaver-Burk plot, and K_T and V_{max} were calculated.

2.5. Bioinformatics

The sequence alignment was performed using the Geneious alignment function (Global Alignment with Cost Matrix Blosum90) in Geneious prime software version 2022.1.1 (Biomatters, Inc., San Diego, CA, USA), and the sequence logo was created using WebLogo version 2.8.2 [41]. NetPhos 3.1 server was used for the prediction and scoring of putative phosphorylation sites, [42], and the 14–3–3-Pred server was used for evaluating potential sites for interaction with 14–3–3 proteins [43]. The PDB-files of 3D models of Trk1 proteins from *S. cerevisiae* and *C. albicans* and Trk2 protein from *S. cerevisiae* were obtained from the AlphaFold database [44,45]; database numbers: P12685, A0A1D8PTL7 and P28584 respectively. The visualization of 3D models and prediction of hydrogen bonds were performed in USFC ChimeraX version 1.1 [46].

2.6. Fluorescence polarization assay

Both *S. cerevisiae* 14–3–3 isoforms (Bmh1 and Bmh2) were expressed and purified as described previously [47,48]. The N-terminal 6 ×His-tag was removed using TEV protease, and final size-exclusion chromatography was performed in a HiLoad Superdex 75 column (GE Healthcare, Chicago, IL, USA). Bmh1 and Bmh2 were dialyzed overnight into a buffer containing 10 mM HEPES (pH 7.4) and 150 mM NaCl. Proteins at an initial concentration of 160 µM, followed by binary dilution series, were incubated for 1 h with 50 nM of FITC-labeled synthetic Trk1 peptide (FITC-RRCFpTLLFP), where pT denotes phosphothreonine (Pepscan Presto BV, Lelystad, Netherlands). The dilution series were performed in 384-well black low-volume flat-bottom plates (Corning, NY, USA) in a buffer containing 10 mM HEPES (pH 7.4), 150 mM NaCl, 0.1% (v/v) Tween 20% and 0.1% (w/v) BSA, using an epMotion P5073 pipetting robot (Eppendorf, Hamburg, Germany). Fluorescence polarization assay was measured using a CLARIOstar microplate reader (BMG Labtech, Thermo Fisher Scientific, Waltham, MA, USA) at 23 °C. The excitation and emission wavelengths were 482 nm and 530 nm, respectively. The K_D values were determined as the mean of four independent measurements.

2.7. Statistics

The obtained data were analysed in Microsoft Excel 2010 or GraphPad Prism version 9.1.0. (GraphPad Software, San Diego, CA, USA). P-values were calculated using the two-tailed Student's T-test in Microsoft Excel 2010. All measurements were repeated at least three times and the mean values with standard deviations are presented.

3. Results

3.1. Involvement of short second intracellular loop (IL2) in the activity regulation and structure integrity of Trk1

To elucidate the mechanism that adapts the activity of Trk1, we centred our study on the identification of putative phosphorylation sites, which might be involved in this process. To narrow down the number of potential candidates (several tens in the whole protein, and 10 of them already confirmed in phosphoproteomic studies, Table S1) we initially focused on the second intracellular loop, IL2. IL2 is only 35 amino-acid residues long (Fig. 1 A) but it contains several Ser and Thr residues that can be phosphorylated. To our knowledge, the role of this short loop has never been studied. When we compared the amino-acid sequences of Trk1 proteins of several yeast species whose Trk1 proteins have been characterized (*S. cerevisiae*, *C. albicans*, *C. glabrata*, *C. dubliniensis*, *C. parapsilosis*, *Z. rouxii*), a remarkably high degree of conservation was observed in IL2 (100% identity for the majority of residues; Fig. 1B and Fig. S1), similarly as in a previous study of *C. albicans* Trk1 protein [49]. Such a degree of conservation among hydrophilic intracellular segments of transporters is rather rare, and suggested a significant function of IL2 in Trk1's activity.

IL2 of *Sc*Trk1 contains 4 prospective phosphorylation sites: Ser878, Ser882, Ser887 and Thr900 (Fig. 1B). Three of them (Ser882, Ser887, Thr900) are fully conserved among the compared sequences, but none of them was identified in previous phosphoproteomic studies (Table S1). When we employed NetPhos 3.1 software [42] to predict and evaluate potential phosphorylation sites on IL2, we obtained substantially high scores for Ser882 and Ser887 (Fig. 1 C). Additionally, three separate algorithms, using 14–3–3 Pred [43] identified Thr900 as a potential site for interaction with 14–3–3 proteins (Fig. 1 C). To unravel the possible contribution of these four residues to the regulation of Trk1, they were individually mutated to alanine, and the resulting versions of Trk1 were expressed from a centromeric vector in BYT12 cells that lacked chromosomal copies of *TRK1* and *TRK2* genes and was consequently unable to grow at low K^+ concentrations.

All four mutants were functional, as they supported the growth of BYT12 cells on 3 mM KCl, similarly to the wild-type Trk1 version (Fig. 2 A). At very low K^+ concentrations, e.g., 50 μM (Fig. 2 A), the growth of cells expressing different Trk1 versions was not the same. Cells expressing the S882A and T900A versions grew slower than the other strains, suggesting a diminished activity of these two mutated Trk1 proteins and, thereby, a role of these residues in upregulating the activity/affinity of Trk1 under K^+ limitation. We also tested growth on plates with the same two concentrations of KCl (50 μM and 3 mM) and supplemented with sodium, lithium, and ammonium salts, or with a pH of 4.0 or 7.2, instead of the usual 5.8 (Fig. S2). The general growth pattern and growth differences were similar to growth observed without added toxic salts; only cells with the Trk1 S882A and T900A versions grew slightly slower on plates with pH 4.0 than on plates with pH 5.8 (Fig. S2). Further, we estimated the initial rate of the uptake of the K^+ analogue Rb^+ in cells starved of K^+ for 1 h (cf. Materials and methods). Due to a negligible Rb^+ uptake in BYT12 cells carrying the empty vector (Fig. 2B), the uptake observed in the other strains corresponded to the activity of Trk1. Fig. 2B shows that Rb^+ uptake was affected to different degrees in cells with all mutated Trk1 versions. The decrease in uptake capacity was more pronounced in BYT12 cells expressing the S882A and T900A versions than in cells harbouring Trk1 with the S878A and S887A mutations, respectively (approximately 35–50% decrease compared to approximately 15% decrease; Fig. 2B).

3.1.1. Role of Ser882 and Thr900

Based on the results of growth tests and Rb^+ uptake measurements, we focused subsequent experiments on cells expressing Trk1 with the substitutions S882A and T900A and estimated the kinetic parameters of Rb^+ uptake via mutated Trk1 versions both in non-starved (NS) and K^+-starved (ST) cells (Fig. 2 C). In non-starved cells, the affinities of wild-type and T900A versions were comparable, while the affinity of S882A decreased by approximately 20%. The maximum velocity was similarly decreased for both mutated Trk1 versions. In K^+-starved cells, in which Trk1 proteins are in the high-affinity state [15], we detected a significantly decreased affinity and maximum velocity for both mutated versions compared to the wild-type Trk1 (Fig. 2 C).

To elucidate whether residues Ser882 and Thr900 contribute to the function of Trk1 similarly, we constructed a Trk1 version with both the S882A and T900A substitutions. The double mutation resulted in additive effects, both in drop tests and Rb^+ uptake measurements (Fig. 2A, B). When we estimated the kinetic parameters of the double mutant, it was evident that it could not reach the high-affinity state, and its transport capacity was also very low (Fig. 2 C). These results suggested that the two residues contribute to the function of Trk1 separately.

To establish a possible connection between the two putative phosphorylation sites (Ser882 and Thr900) and specific kinases, we decided to express both wild-type and mutated versions in BYT12 cells with deletion of the open reading frames for the kinases Hog1, Snf1, Sky1, Ptk2 and Hal5. As was mentioned in the Introduction, the kinases Snf1, Sky1 and Hal5 are thought to play a role in the regulation of Trk1. The Ptk2 kinase was included, as it activates the Pma1 H^+-ATPase [50] and may thus have an important role in the interplay between the function of Pma1 and Trk1. Finally, as the Hog1 pathway is involved in the stress response related to cation homeostasis [51], we hypothesised that Hog1 kinase could have a stimulatory effect on Trk1 as well. As shown in Fig. S3, we detected an overall negative effect of *HOG1* and *SNF1* deletions on the growth of BYT12 cells expressing all three Trk1 versions, while the deletion of *SKY1*, *PTK2* and *HAL5* had no apparent effect. As the differences in growth between cells expressing wild-type and mutant Trk1 versions were not diminished in strains lacking the kinases (as a consequence of non-phosphorylated residues of the wild-type Trk1), it seemed likely that none of the tested kinases was involved in the regulation of Trk1's activity via the phosphorylation of Ser882 and Thr900 under the conditions of our experiments.

Besides involvement in the regulation of the transporter's affinity, Ser882 and Thr900 may also have a function in protein structure and, thereby, in its biogenesis and stability. To inform on a potential role versus other roles, we introduced additional substitutions for each residue. These were replacements with aspartic acid, with its negatively-charged side chain presumably able to mimic phosphorylated residues (an approach previously applied in [52,53]), and with cysteine, whose side chain is structurally similar to both serine and threonine and at the same time cannot be phosphorylated. We presumed that if the substitution for aspartic acid could reverse the negative effect of the substitution for alanine, then residues would most likely be targets for activating phosphorylation, and on the other hand, if the cysteine residue gave functionality, Ser882 and Thr900 residues could possibly fulfil more a structural function.

As shown in Fig. 3A, the replacement with cysteine did not result in a negative effect on the growth of cells at low external K^+ concentrations. On the other hand, the replacement with aspartic acid had the same or even a slightly more pronounced (T900D vs. T900A, Fig. 3A) effect than the introduction of alanine. We did not detect any additional differences when the growth under the presence of toxic salts or low and high pH was tested. Cells with the S882D and
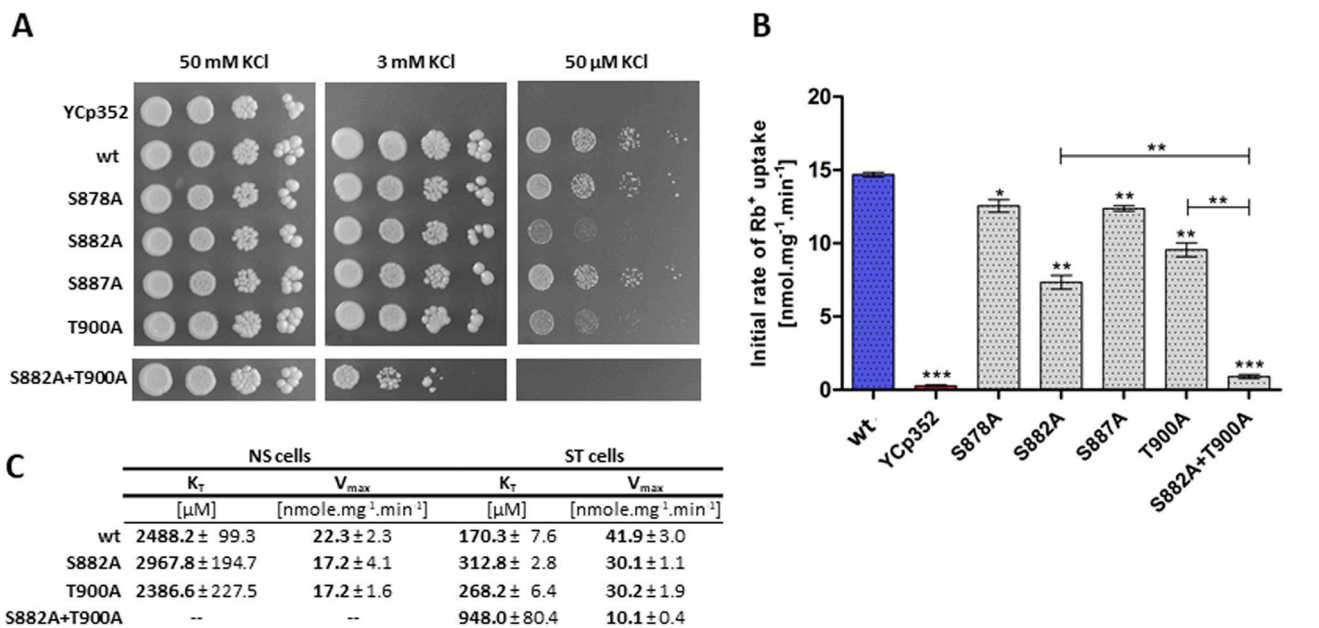
	NS cells		ST cells	
	K_T	V_{max}	K_T	V_{max}
	[µM]	[nmole.mg^{-1}.min^{-1}]	[µM]	[nmole.mg^{-1}.min^{-1}]
wt	2488.2 ± 99.3	22.3 ± 2.3	170.3 ± 7.6	41.9 ± 3.0
S882A	2967.8 ± 194.7	17.2 ± 4.1	312.8 ± 2.8	30.1 ± 1.1
T900A	2386.6 ± 227.5	17.2 ± 1.6	268.2 ± 6.4	30.2 ± 1.9
S882A+T900A	--	--	948.0 ± 80.4	10.1 ± 0.4

Fig. 2. Replacements of Ser878, Ser882, Ser887 and Thr900 with alanine affect the activity of Trk1. (A) Growth of *trk1Δ trk2Δ* (BYT12) cells carrying an empty vector (YCp352) or expressing wild-type (wt) Trk1 and its mutated versions on YNB-F plates supplemented with indicated concentrations of KCl. Images were captured after 7 days of incubation at 30 °C. (B) Initial rates of 100 µM Rb$^+$ uptake in cells starved of K$^+$ for 1 h in YNB-F (*, $p < 0.05$; **, $p < 0.01$; ***, $p < 0.001$). (C) Kinetic parameters of Rb$^+$ uptake via wild-type (wt) Trk1 and its mutated versions. Cells were grown overnight in YNB supplemented with 100 mM KCl (non-starved cells, NS) or additionally incubated in YNB-F for 1 h (K$^+$-starved cells, ST).

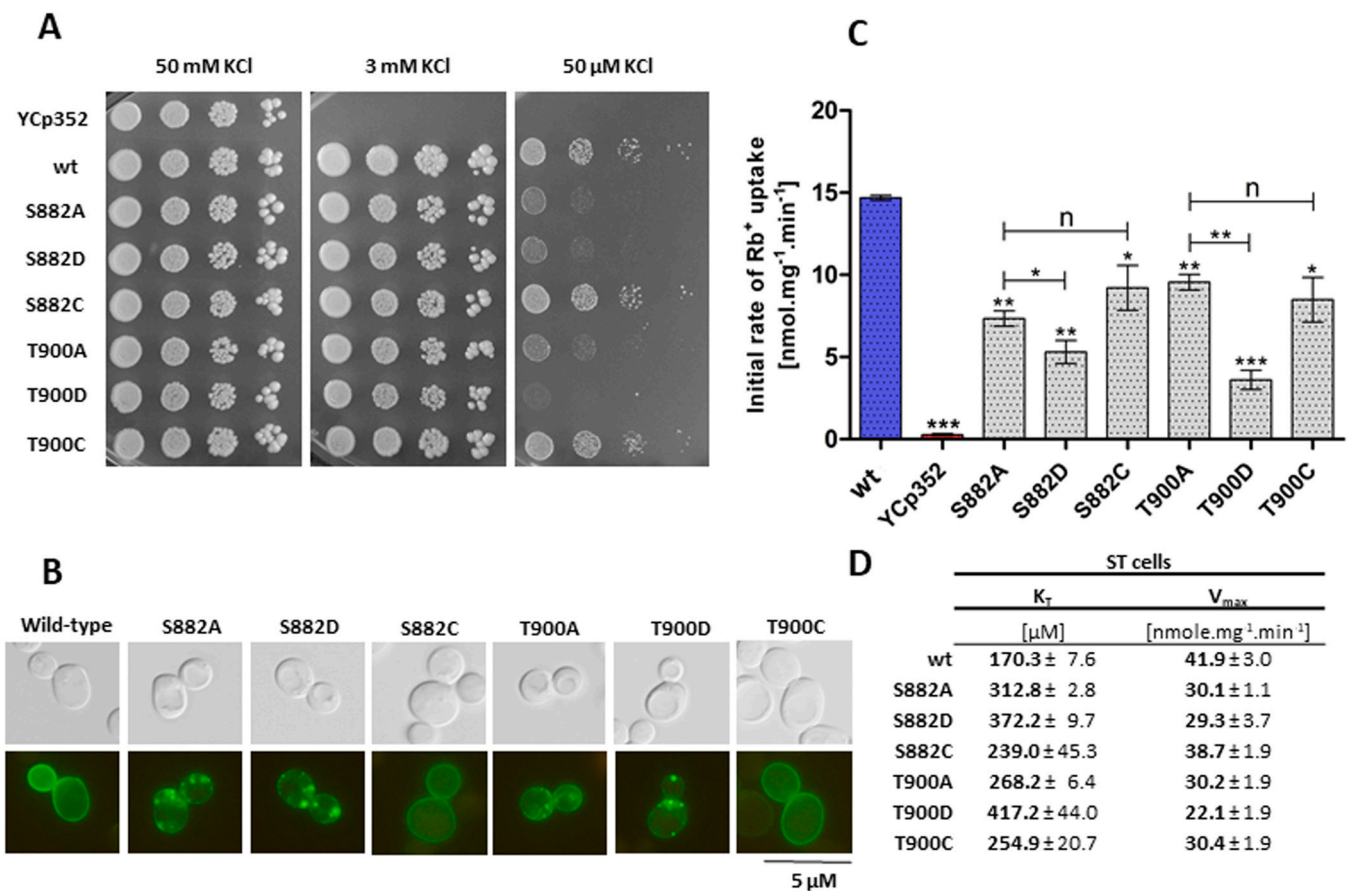|	ST cells	
	K_T	V_{max}
	[µM]	[nmole.mg^{-1}.min^{-1}]
wt	170.3 ± 7.6	41.9 ± 3.0
S882A	312.8 ± 2.8	30.1 ± 1.1
S882D	372.2 ± 9.7	29.3 ± 3.7
S882C	239.0 ± 45.3	38.7 ± 1.9
T900A	268.2 ± 6.4	30.2 ± 1.9
T900D	417.2 ± 44.0	22.1 ± 1.9
T900C	254.9 ± 20.7	30.4 ± 1.9

Fig. 3. S882C and T900C do not exhibit the negative effects of S882A and T900A. (A) Growth of BYT12 cells carrying empty vector (YCp352) or expressing wild-type (wt) Trk1 and its mutated versions on YNB-F plates supplemented with indicated concentrations of KCl. Images were captured after 7 days of incubation at 30 °C. (B) Localization of GFP-tagged wild-type Trk1 and its mutated versions in BYT12 cells. (C) Initial rates of 100 µM Rb$^+$ uptake in cells starved of K$^+$ for 1 h in YNB-F (*, $p < 0.05$; **, $p < 0.01$; ***, $p < 0.001$; n, no significant difference). (D) Kinetic parameters of Rb$^+$ uptake via wild-type (wt) Trk1 and its mutated versions in cells K$^+$-starved in YNB-F for 1 h (ST cells).

T900D versions were a little more sensitive to low pH (Fig. S4), similarly to cells with the S882A and T900A versions of Trk1.

When we tagged the wild-type and mutated Trk1 versions C-terminally with GFP, expressed them from a multicopy plasmid and visualized the cells under a fluorescence microscope, we observed a dramatic effect of the S882A/D and T900A/D substitutions. A major portion of these mutated versions was not located in the plasma membrane, but in several spots inside the cells (Fig. 3B). The subcellular localization of cysteine-containing versions was similar to the plasma-membrane localization of wild-type Trk1 (Fig. 3B) and suggested that the observed restoration of the relative good growth of cells with the S882C and T900C versions (Fig. 3 A, 50 µM KCl) was a consequence of the increased amount of Trk1 with cysteines in the plasma membrane. The presence of a cysteine may lead to new disulfide bridges stabilizing the active state of Trk1 or favoring tetramer formation.

Based on the results from drop tests (Fig. 3 A) and fluorescence microscopy (Fig. 3B), we expected a substantially increased rate of Rb^+ uptake in cells expressing Trk1 S882C and T900C compared to cells with the S288A/D and T900A/D versions. But surprisingly, the initial uptake rates of 100 µM Rb^+ in cells expressing Trk1 versions with alanine and cysteine substitutions were similar, and only those with aspartate substitutions were significantly lower (Fig. 3 C). Similarly, when we estimated the kinetic parameters for Rb^+ uptake, the differences between them were much lower than expected from the drop tests and fluorescence microscopy (Fig. 3D). The results obtained in Rb^+ uptake measurements suggested first that all the mutants, including those with cysteine, might have a lower affinity for Rb^+ than the wild-type Trk1, and second, that probably a substantial proportion of wild-type, S882C and T900C Trk1 molecules in the plasma membrane is not in an active state, as deduced from relatively small differences in the maximum velocities of individual transporters (Fig. 3D) and considerable differences in their localization in cells (Fig. 3B).

3.1.2. Model structure of the IL2

To broaden our knowledge about the putative role of the short IL2 in the structure and function of Trk1, we analyzed its AlphaFold 3D model [44]. We could not use the latest published model, as it lacks internal segments of the Trk1 protein and focuses exclusively on MPM domains [12]. Fig. 4 A shows that the IL2 is a highly ordered segment with two helical regions (residues 869–877 and 883–893, respectively) connected by a short turn (residues 878–882). These two helical regions explain the remarkable degree of conservation observed in the comparison of Trk1 sequences from various yeast species (Fig. 1B, S1), and also point to the potentially crucial function of this segment for the function of Trk1. We also observed a very similar conformation of IL2 in models of *S. cerevisiae* Trk2 and *C. albicans* Trk1 (Fig. 4B).

The proper conformation of the two helices and the entire region is presumably maintained by a number of non-covalent interactions including hydrogen bonds. Fig. 4C shows the participation of the studied residues Ser878, Ser882, Ser887 and Thr900 in the formation of such hydrogen bonds, and potentially explains the distinct effects of the substitution of residues 878 and 887 for alanine compared to the same substitution of residues 882 and 900. As is visible in Fig. 4C, both Ser878 and Ser887 only participate in the creation of hydrogen bonds with their main chains and not the side chains (left panels), whereas Ser882 and Thr900 participate in the formation of hydrogen bonds with their side chains (right panels). The fact that the side chain of alanine is unable to form hydrogen bonds could explain the relatively strong negative effect of the introduction of alanine into positions 882 and 900, and the marginal effects of alanine at positions 878 and 887 (Fig. 2A, B). As shown in the upper right panel of Fig. 4C, the side chain of Ser882 forms a hydrogen bond with Glu886 from the very beginning of the second

helical region of IL2, suggesting the importance of this interaction in stabilizating the orientation of the second IL2-helix with respect to the short turn connecting it to the first helical region. Residue Thr900, on the other hand, forms a hydrogen bond with His122 of the second transmembrane helix of the MPM1 domain (Fig. 4C, lower right panel). This interaction could participate in the stabilization of not only local but also the overall conformation of the Trk1 protein. The ability of the side chain of cysteine to form hydrogen bonds combined with its high structural similarity to the side chains of amino acids with hydroxyl groups may thus explain the minor effect of cysteine in positions 882 and 900 on growth on low K^+ and subcellular localization (Fig. 3A, B).

The structural importance of residues Ser882 and Thr900 probably also explains the failure of mimicking putative phosphorylation by replacing them with aspartic acid, as the presence of a large negative charge in structurally important regions of Trk1 during the folding of the nascent protein might lead to structural impairments and thus to mislocalization of the protein. To confirm this hypothesis, we introduced a negative charge (aspartyl residue) to position 881 instead of leucine, the side chain of which, according to the model, points outward from the turn of IL2, and does not participate in the formation of non-covalent interactions (Fig. S5B). As shown in Fig. S5A, this substitution had no effect on the growth of cells on low K^+, this is consistent with our hypothesis that a negatively charged residue at position 882 disrupts structurally crucial non-covalent interactions and consequently leads to improper folding and mislocalization of the protein.

3.2. Involvement of 14–3-3 proteins in the regulation of Trk1

As Thr900 was predicted to be a potential site for interaction with 14–3-3 proteins (Fig. 1C), we examined the involvement of 14–3-3 proteins in K^+ uptake and homeostasis. We expressed wild-type Trk1 in a strain that, besides *TRK1* and *TRK2,* also lacks the *BMH1* gene (BYT12Δ*bmh1*), which accounts for about 80% of 14–3-3 proteins. Fig. 5A shows that the deletion of *BMH1* resulted in a slightly diminished growth of cells at 50 µM KCl, suggesting the role of 14–3-3 proteins in Trk1 upregulation in these conditions. At higher KCl concentrations, the absence of Bmh1 had no effect on cell growth (Fig. 5).

The deletion of *BMH1* also led to a very slight decrease in Rb^+ uptake (Fig. 5C) but not to a changed localization of the Trk1 in cells (Fig. 6C). A detailed analysis of Trk1's kinetic parameters revealed that the absence of Bmh1 changed the transporter's affinity (Fig. 5D). In K^+-starved cells without Bmh1, Trk1 did not reach its maximum affinity, which corresponds to the observed difference in cell growth at low K^+. Taken together, the results obtained with the BYT12Δ*bmh1* strain suggested the involvement of 14–3-3 proteins in the regulation of K^+ homeostasis, probably via interaction with Trk1.

To elucidate in more detail a possible connection between Trk1 and 14–3-3 proteins, we next focused on identifying putative binding sites in the Trk1 protein, other than T900, which was identified in the first search. Again employing the three prediction algorithms of the 14–3-3-Pred software, we identified 14 potentially interacting residues (listed in Table S6). For further analysis, we selected 8 residues, 7 of them according to two additional parameters, a NetPhos 3.1 score above 0.6, and more than 40% identity to other Trk sequences. The eighth residue, Thr491, even though it did not fulfil all the requirements, was included as a neighbour of Ser490. The 8 selected residues were mutated to alanine, and mutated Trk1 proteins were expressed in BYT12 cells.

When the growth of cells expressing these 8 mutated Trk1 versions was tested on plates supplemented with various concentrations of KCl, most of the mutants gave the same phenotype as the wild-type Trk1, and only cells expressing Trk1 T900A grew slower at very low K^+ concentrations (Fig. 6A). However, when the Rb^+ uptake
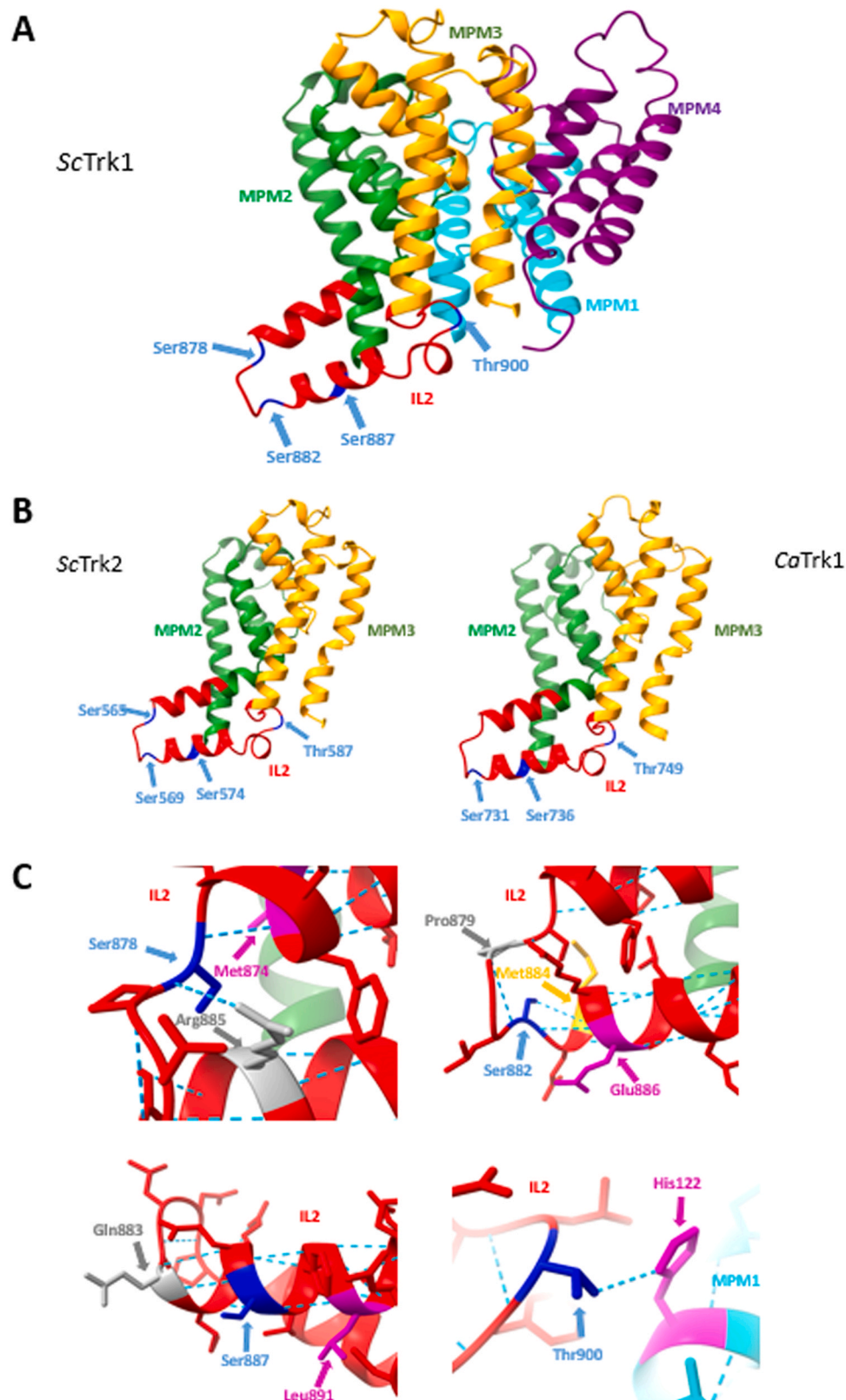
Fig. 4. 3D model of Trk1 depicting structure of IL2 and predicted hydrogen bonds. PDB files were obtained from the AlphaFold database and visualized in ChimeraX version 1.1. (A) IL2 and MPM domains of *S. cerevisiae* Trk1 (database number P12685) in red. Putative phosphorylation sites of IL2 are highlighted with blue arrows. (B) IL2 of *S. cerevisiae* Trk2 (left, database number P28584) and IL2 of *C. albicans* Trk1 (right, database number A0A1D8PTL7) in red. For better clarity, only the MPM2 (green) and MPM3 (yellow) are shown. Putative phosphorylation sites of IL2 are highlighted with blue arrows. (C) Hydrogen bonds of Ser878 (blue) of IL2 with Met874 and Arg885 (upper left panel), Ser882 (blue) of IL2 with Pro879, Met884 and Glu886 (upper right panel), Ser887 (blue) of IL2 with Gln883 and Leu891 (bottom left panel), and Thr900 (blue) of IL2 with His122 (bottom right panel).
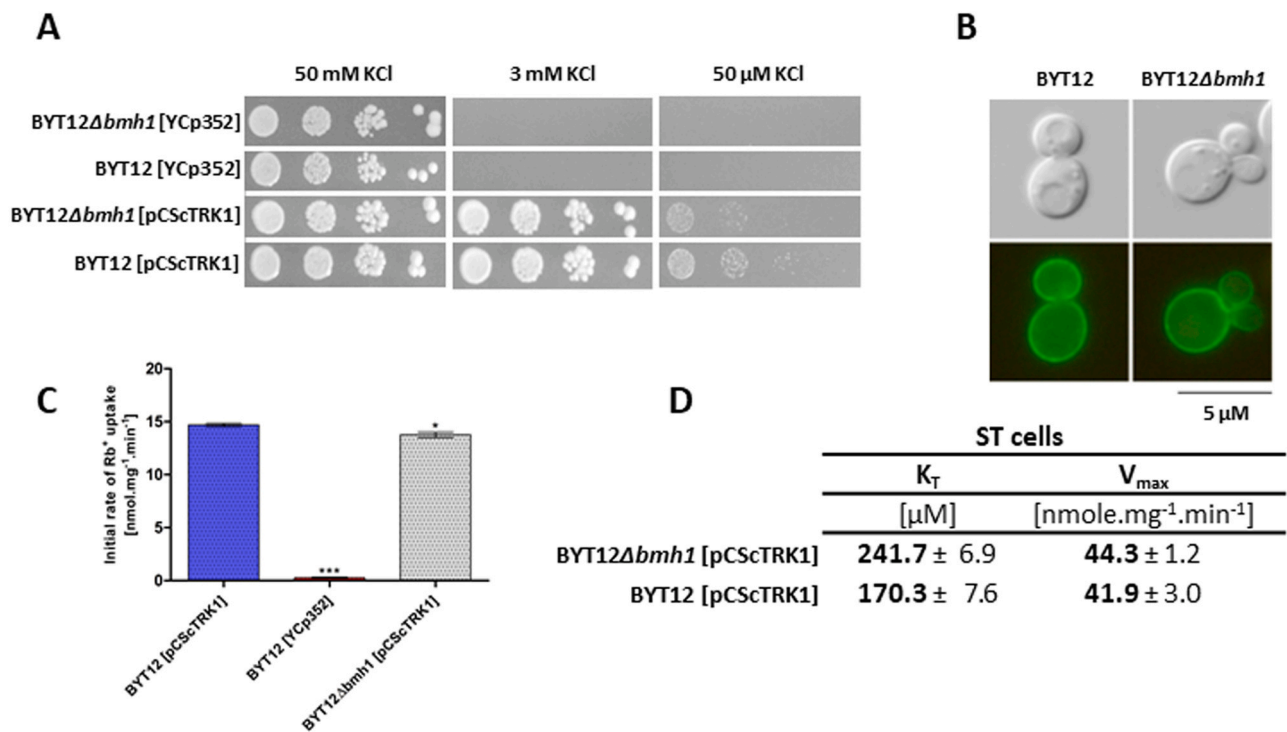
Fig. 5. Involvement of 14–3–3 proteins in K+ uptake and homeostasis. (A) Growth of BYT12 and BYT12Δ*bmh1* cells carrying an empty vector (YCp352) or pCScTRK1 on YNB-F plates supplemented with indicated concentrations of KCl. Images were captured after 5 days of incubation at 30 °C. (B) Subcellular localization of GFP-tagged Trk1 in BYT12 and BYT12Δ*bmh1* cells. (C) Initial rates of 100 µM Rb+ uptake in cells starved of K+ for 1 h in YNB-F (*, p < 0.05; ***, p < 0.001). (D) Kinetic parameters of Rb+ uptake via Trk1 in BYT12 and BYT12Δ*bmh1* cells starved of K+ in YNB-F for 1 h (ST cells).

was measured, three mutants exhibited a significantly decreased uptake. In addition to Trk1 T900A, also cells expressing Trk1 T155A and S414A (residues located in the first long intracellular loop) accumulated approximately 25% less Rb+ than the wild-type Trk1 (Fig. 6B). Unlike Trk1 T900A, both versions were localized to the plasma membrane (Fig. 6C), and thus the observed decrease in Rb+ uptake was most likely caused by a change in the activity of the protein rather than in its mislocalization. When kinetic parameters of Rb+ uptake in K+-starved BYT12 cells expressing mutated version were estimated, T155A and S414A substitutions led to a slight decrease in affinity, while there were no significant changes in maximum velocity (Fig. 6D). The obtained results confirmed that T900 is, of the residues predicted to be 14–3–3 binding sites, the most important for Trk1 localization and activity under low K+ conditions.

We also examined the possibility of physical interaction between 14-3-3 proteins and Trk1 in an in vitro study. First, a short synthetic peptide containing phosphorylated Thr900 bordered on each side by the four amino acids from the natural sequence of Trk1 (RRCFpTLLFP) was synthesized. The peptide was labelled on its N-terminus with fluorescein isothiocyanate (FITC), and a fluorescence polarization assay was performed to determine binding affinities to both Bmh1 and Bmh2 as described in Materials and methods. Fig. 7A shows that the phosphopeptide interacts with both Bmh1 and Bmh2 in a dose-dependent manner. Binding affinities for interaction with Bmh1 and Bmh2 were relatively high, with dissociation constants of 4.0 and 3.4 µM, respectively (Fig. 7B).

In summary, the obtained results confirmed that Bmh1 and Bmh2 bind to Thr900 of Trk1, consistently with their involvement in the regulation of activity and/or localization of Trk1, and this way in K+ homeostasis. Moreover, we identified two new residues in IL1, Thr155 and Ser414, as potentially interacting with 14–3–3 proteins and thereby involved in regulating Trk1, though they are not as important as Thr900 at low K+ conditions.

4. Discussion

Trk1 is expressed constitutively and at a low level, at both high and low external K+ concentrations, thus its activity must be precisely regulated at the protein level to ensure optimum K+ concentration in the cell and to compensate properly for the changes in the efflux of positive charges protons via Pma1 [24]. As phosphorylation is the dominant posttranslational modification in eukaryotic cells [54], we focused on the role of potentially phosphorylated amino-acid residues in the transporter's activity. Due to intracellular segments making up more than 70% of the protein (881 amino-acid residues out of 1235), Trk1 contains a large abundance of potential phosphorylation sites. We therefore limited our study to a specific subset of these sites, putative phosphorylation sites in the highly conserved second intracellular loop (IL2) and putative phosphorylation sites with the potential for interaction with 14–3–3 proteins.

Apart from harbouring four potential phosphorylation sites, IL2 of Trk1 is a highly structured domain with two helical subdomains (Fig. 4), according to a model acquired from the AlphaFold database. High degree of conservation of this domain (Fig. 1B and Fig. S1) strongly suggests its functional importance. Cytosolic domains of transport proteins were shown to be involved in activity regulation in various ways, most notably by interaction with either ATP [55] or with other proteins regulating a given transporter [56]. Moreover, a structurally similar element was proposed to be involved in the gating of KtrB, an ion channel that structurally belongs to the same group of SKT-proteins as Trk1 [56].

Two out of four potential phosphorylation sites of IL2, Ser878 and Ser887, seem to not be very important for Trk1 transport activity under our experimental conditions. Their replacement with alanine did not result in a substantial phenotype of growth at low K+ (Fig. 2A), and the ability of mutated Trk1 versions to transport Rb+ was only slightly affected (Fig. 2B). On the other hand, analysis of the two other residues, Ser882 and Thr900, revealed a dual function,
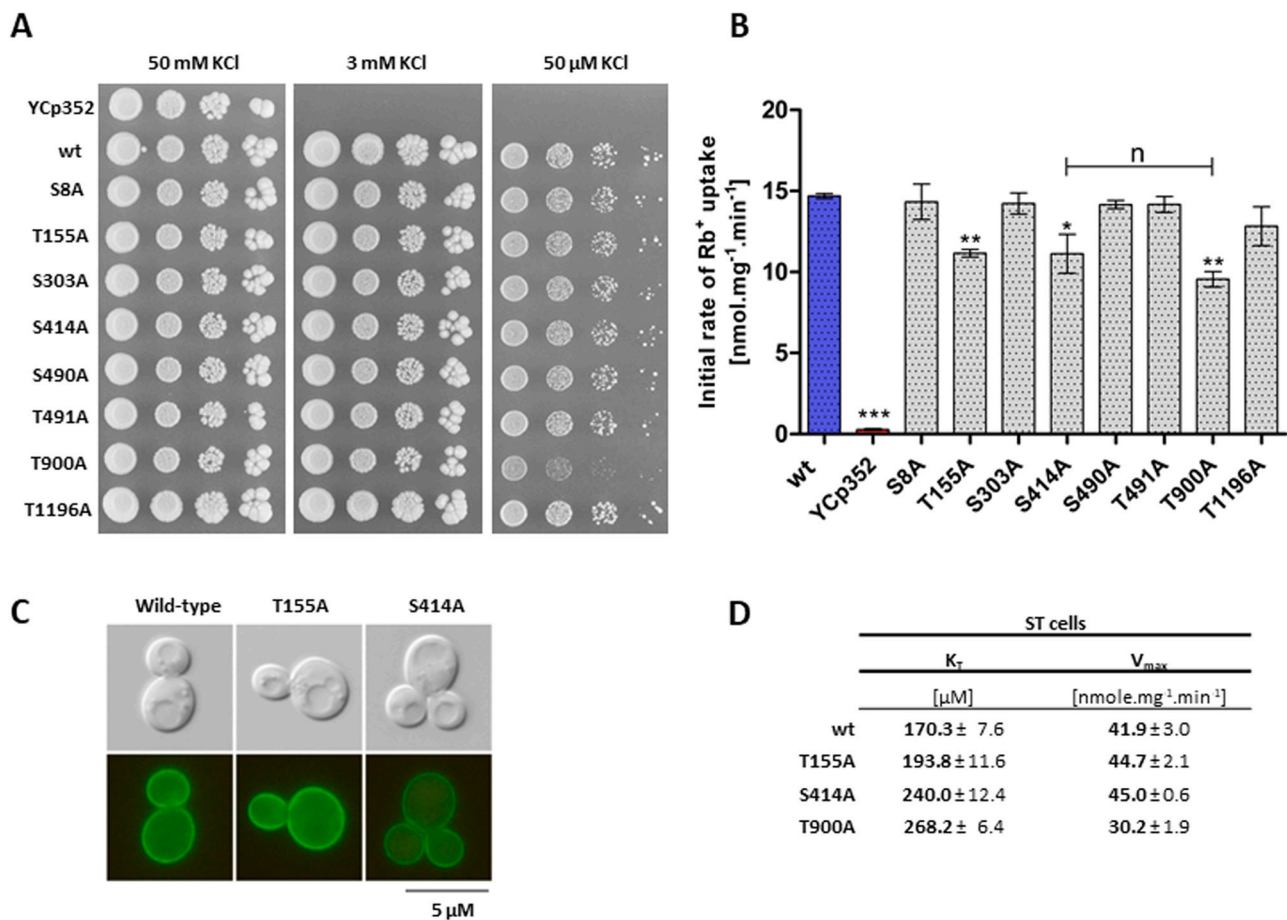
Fig. 6. Effect of mutation of putative sites for interaction with 14–3–3 proteins. (A) Growth of BYT12 cells carrying empty vector (YCp352) or expressing wild-type (wt) Trk1 and its mutated versions on YNB-F plates supplemented with indicated concentrations of KCl. Images were captured after 7 days of incubation at 30 °C. (B) Initial rates of 100 μM Rb$^+$ uptake in cells starved of K$^+$ for 1 h in YNB-F (*, $p < 0.05$; **, $p < 0.01$; ***, $p < 0.001$; n, no, significant difference). (C) Localization of GFP-tagged wild-type Trk1 and its mutated versions in BYT12 cells. (D) Kinetic parameters of Rb$^+$ uptake via wild-type (wt) Trk1 and its mutated versions. Cells were K$^+$-starved in YNB-F for 1 h (ST cells).

both structural and activity-regulating ones. Upon their replacement with alanine, cells harbouring Trk1 versions with these mutations grew very slowly on low K$^+$ (Fig. 2A), Trk1 in these cells did not reach its highest affinity at low K$^+$ conditions, and the maximum velocity was significantly diminished (Fig. 2C). The decrease in maximum velocity was most likely a consequence of mislocalisation of a significant portion of the mutated proteins (Fig. 3B).

As was mentioned above, IL2 is highly structured (Fig. 4A), and many of its residues are predicted to participate in noncovalent interactions with other MPM domains or intracellular segments of Trk1 (Fig. 4C and Fig. S6). Ser882 and Thr900 probably fulfil crucial

structural functions. According to the model, they both participate in the formation of hydrogen bonds, and their replacement with alanine (eliminating some hydrogen bonds) leads to mislocalized Trk1 proteins (Fig. 3B). The structural function of these two residues is also supported by the lack of negative effects upon the introduction of cysteine (Fig. 3A, B). The non-covalent interactions of Ser882 and Thr900 might be especially important for proper folding during the synthesis of a nascent protein, which is consistent with the failure of mimicking a phosphorylation by the introduction of a negatively charged aspartic acid (Fig. 3). Aspartyl's negative charge, when placed at position 882 or 900 in IL2, during the synthesis of a Trk1
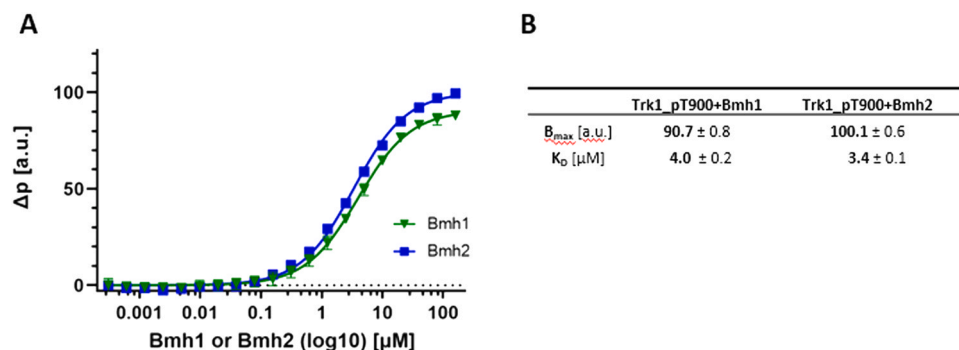

Fig. 7. *In vitro* interaction between pThr900 and Bmh proteins. (A) Fluorescence polarization (FP) assay of FITC-labelled peptide RRCFpTLLFP with phosphorylated Thr900 (Trk1_pT900) titrated with Bmh1 or Bmh2. (B) Parameters (K$_D$ and B$_{max}$) of Trk1_pT900 peptide binding to Bmh1 (Trk1_pT900 +Bmh1) and Bmh2 (Trk1_pT900 +Bmh2). The binding affinities were determined by fitting the FP data to a one-site-binding model. All data points are the mean ± SD of four replicates.

might lead to folding impairments and consequent mislocalization [57]. This is supported by the fact that the introduction of an aspartyl residue at position 881 (mutation L881D, Fig. S5), where its side chain points outward from the turn of IL2, has no negative effect on Trk1 activity. As for the second role of the studied Ser882 and Thr900 residues, a change in their phosphorylation status (in an already fully folded protein in the plasma membrane), may lead to changes to existing hydrogen bonds or to the formation of new ionic interactions [58], which in turn affect the conformation of IL2, and the activity and affinity of the transporter.

Taken together, the obtained results revealed a potential dual function of residues Ser882 and Thr900. The structural function of Ser882 and Thr900 residues, ergo their importance for the proper folding and conformation of Trk1, is supported 1) by a substantial degree of mislocalization upon their replacement with alanine, and the absence of this mislocalization upon replacement with a cysteine (Figs. 3B), and 2) by putative non-covalent interactions of their side chains (Fig. 4 C). Given the observed decreased Rb$^+$ uptake capacity of Trk1 versions with cysteine, it is possible that residues Ser882 and Thr900 are also targets for phosphorylation that upregulates Trk1 activity. Since the decrease in Rb$^+$ uptake was more visible in K$^+$-starved cells (Fig. 2 C), the potential phosphorylation of the two residues would most likely occur under K$^+$ limitations.

One of the consequences of the phosphorylation status of a protein is the possibility of binding 14–3–3 regulatory proteins. As is mentioned in the Introduction, yeast 14–3–3 proteins Bmh1 and Bmh2 are involved in numerous cellular processes, and there were a few pieces of evidence that 14–3–3 proteins could be involved in the maintenance of K$^+$ homeostasis, e.g. via inhibiting one of the K$^+$ exporters, Nha1 (which is also expressed at a constitutive and low level, similarly to Trk1) [35]. Our experiments also showed that the absence of Bmh1 had a slightly negative effect on the growth of cells at limited concentrations of K$^+$ (50 μM KCl; Fig. 5A), and prevented the highest affinity for Rb$^+$ uptake via Trk1 from being reached (Fig. 5D). All this prompted us to study the possibility of 14–3–3 involvement in the regulation of Trk1 activity. In addition to Thr900, a further 13 candidate residues were identified using the prediction software (Table S6); two of them (Thr155 and Ser414) were also identified in phosphoproteomic studies (Table S1) as being likely to be phosphorylated under stress conditions [17,19]. When we mutated 8 selected residues to alanine and expressed them in BYT12, it was evident that, apart from T900A, only 2 mutations (T155A and S414A) resulted in a phenotype change (lower uptake of Rb$^+$; Fig. 6B). In general, under stress, an increased K$^+$ uptake is favourable for cell survival, thus the phosphorylation of both Thr155 and Ser414 and consequent interaction with 14–3–3 proteins could have a stimulatory effect on the function of Trk1, and the impossibility of this interaction would decrease the transport capacity of Trk1, as can be seen in our results (Fig. 6B, D). Similarly, phosphorylated Thr900 is a site of interaction with both Bm1 and Bmh2 proteins, as shown not only in whole-cell experiments (Fig. 6) but also confirmed by in vitro measurement (Fig. 7).

The study of the connection between Trk1 and 14–3–3 proteins was partially aimed at identifying a regulatory link between the K$^+$ importing and exporting activity necessary to avoid a futile cycle of K$^+$ uptake via Trk1 and efflux via Nha1 under low K$^+$ conditions. Our results showing the stimulatory effect of 14–3–3 proteins on the activity of Trk1 support the hypothesis about the 14–3–3-mediated interplay between Nha1 and Trk1 activities. In addition to Nha1, 14–3–3 proteins could, in theory, also represent a regulatory connection between Trk1 and H$^+$-ATPase Pma1, which is responsible for the export of protons. As was previously shown, there is a simultaneous activation of Trk1 and Pma1, as the import of K$^+$ needs to be balanced by the export of protons in order to maintain proper membrane potential and vice versa [11, 24, 59]. Pma1 ATPase has been shown to be regulated by a C-terminus-mediated

autoinhibition suppressed by phosphorylation [60]. A strikingly similar mechanism has been described for a plant H$^+$-ATPase, in which 14–3–3 proteins play a role [36,61]. It is possible that 14–3–3 proteins upregulate the activity of yeast H$^+$-ATPase Pma1 by suppressing this autoinhibition in a similar way as in plant H$^+$-ATPase. Bmh1 and Bmh2 proteins could thus represent a regulatory link connecting at least three important players in K$^+$ homeostasis (Trk1, Nha1 and Pma1). For instance, under conditions of K$^+$ limitation, the phosphorylation and subsequent binding of 14–3–3 proteins could lead to a simultaneous stimulation of K$^+$ acquisition via Trk1, balancing the membrane potential by Pma1 activation, and retention of the acquired K$^+$ by reduction of Nha1 activity.

5. Conclusions

This study newly identified the second, very short and conserved, intracellular loop as a highly structured segment involved in the proper biogenesis of *S. cerevisiae* Trk1, and its two residues Ser882 and Thr900 as important both for the protein's biogenesis and, probably upon phosphorylation, for the upregulation of Trk1′s affinity under potassium limitation. Additionally, the role of 14–3–3 proteins Bmh1 and Bmh2 in the regulation of K$^+$ uptake was demonstrated, and the binding of 14–3–3 proteins to Thr900 was confirmed by in vitro experiments.

CRediT authorship contribution statement

Jakub Masaryk: Conceptualization, Investigation, Writing – original draft; **Deepika Kale:** Investigation; **Pavel Pohl:** Investigation, Data curation; **Francisco J. Ruiz-Castilla:** Methodology, Investigation; **Olga Zimmermannová:** Methodology, Funding acquisition, Writing – review & editing; **Veronika Obšilová:** Conceptualization, Supervision, Writing – review & editing, **José Ramos**: Methodology, Supervision, Funding acquisition; **Hana Sychrová:** Conceptualization, Supervision, Writing – original draft, Writing – review & editing, Funding acquisition.

Declaration of Competing Interest

The authors declare that they have no known competing financial interests or personal relationships that could have appeared to influence the work reported in this paper.

Acknowledgements

Appendix A. Supporting information

Supplementary data associated with this article can be found in the online version at doi:10.1016/j.csbj.2023.04.019.

References

[1] Arino J, Ramos J, Sychrova H. Alkali metal cation transport and homeostasis in yeasts. Microbiol Mol Biol Rev 2010;74(1):95–120. https://doi.org/10.1128/MMBR.00042-09

[2] Arino J, Ramos J, Sychrova H. Monovalent cation transporters at the plasma membrane in yeasts. Yeast 2019;36(4):177–93. https://doi.org/10.1002/yea.3355

[3] Sasikumar A, Killiea D, Kennedy B, Brem R. Potassium restriction boosts vacuolar acidity and extends lifespan in yeast. Exp Gerontol 2019;120:101–6. https://doi.org/10.1016/j.exger.2019.02.001

[4] Ramos J, Arino J, Sychrova H. Alkali-metal-cation influx and efflux systems in nonconventional yeast species. FEMS Microbiol Lett 2011;317(1):1–8.

[5] Ruiz-Castilla F, Bieber J, Caro G, Michan C, Sychrova H, Ramos J. Regulation and activity of CaTrk1, CaAcu1 and CaHak1, the three plasma membrane potassium transporters in Candida albicans. Biochim Biophys A 2021;1863(1):83486. https://doi.org/10.1016/j.bbamem.2020.183486

[6] Gaber R, Styles C, Fink G. TRK1 encodes a plasma membrane protein required for high-affinity potassium transport in Saccharomyces cerevisiae. Mol Cell Biol 1988;8(7):2848–59. https://doi.org/10.1128/mcb.8.7.2848-2859.1988

[7] Petrezselyova S, Ramos J, Sychrova H. Trk2 transporter is a relevant player in K+ supply and plasma-membrane potential control in Saccharomyces cerevisiae. Folia Microbiol 2011;56(1):23–8. https://doi.org/10.1007/s12223-011-0009-1

[8] Borovikova D, Herynkova P, Rapoport A, Sychrova H. Potassium uptake system Trk2 is crucial for yeast cell viability during anhydrobiosis. FEMS Microbiol Lett 2014;350(1):28–33. https://doi.org/10.1111/1574-6968.12344

[9] Dušková M, Cmunt D, Papoušková K, Masaryk J, Sychrová H. Minority potassium-uptake system Trk2 has a crucial role in yeast survival of glucose-induced cell death. Microbiology 2021;167:001065. https://doi.org/10.1099/mic.0.001065

[10] Bertl A, Ramos J, Ludwig J, Lichtenberg-Frate H, Reid J, Bihler H, Calero F, Martinez P, Ljungdahl P. Characterization of potassium transport in wild-type and isogenic yeast strains carrying all combinations of trk1, trk2 and tok1 null mutations. Mol Microbiol 2003;47(3):767–80. https://doi.org/10.1046/j.1365-2958.2003.03335

[11] Navarrete C, Petrezselyova S, Barreto L, Martinez Z, Zahradka J, Arino J, Sychrova H, Ramos J. Lack of Main K+ uptake systems in Saccharomyces cerevisiae cells affects yeast performance in both potassium-sufficient and potassium-limiting conditions. FEMS Yeast Res 2010;10(5):508–17. https://doi.org/10.1111/j.1567-1364.2010.00630

[12] Zayats V, Stockner T, Pandey S, Wortz K, Ettrich R, Ludwig J. A refined atomic scale model of the Saccharomyces cerevisiae K+-translocation protein Trk1p combined with experimental evidence confirms the role of selectivity filter glycines and other key residues. Biochim Biophys A 2015;1848(5):1183–95. https://doi.org/10.1016/j.bbamem.2015.02.007

[13] Kale D, Spurny P, Shamayeva K, Spurna K, Kahoun D, Ganser D, Zayats V, Ludwig J. The S. cerevisiae cation translocation protein Trk1 is functional without its "long hydrophilic Loop" But LHL regulates cation translocation activity and selectivity. Biochim Biophys A 2019;1861(8):1476–88. https://doi.org/10.1016/j.bbamem.2019.06.010

[14] Rivetta A, Slayman C, Kuroda T. Quantitative modeling of chloride conductance in yeast TRK potassium transporters. Biophys J 2005;89(4):2412–26. https://doi.org/10.1529/biophysj.105.066712

[15] Masaryk J, Sychrova H. Yeast Trk1 potassium transporter gradually changes its affinity in response to both external and internal signals. J Fungi 2022;8(5):432. https://doi.org/10.3390/jof8050432

[16] Helbig A, Rosati S, Pijnappel P, van Breukelen B, Timmers M, Mohammed S, Slijper M, Heck A. Perturbation of the yeast N-acetyltransferase NatB induces elevation of protein phosphorylation levels. BMC Genom 2010;11:685. https://doi.org/10.1186/1471-2164-11-685

[17] Li X, Gerber S, Rudner A, Beausoleil S, Haas W, Villén J, Elias J, Gygi S. Large-scale phosphorylation analysis of alpha-factor-arrested Saccharomyces cerevisiae. J Proteome Res 2007;6(3):1190–7. https://doi.org/10.1021/pr060559j

[18] Albuquerque C, Smolka M, Payne S, Bafna V, Eng J, Zhou H. A multidimensional chromatography technology for In-depth phosphoproteome analysis. Mol Cell Proteom 2008;7:1389–96. https://doi.org/10.1074/mcp.M700468-MCP200

[19] Swaney D, Beltrao P, Starita L, Guo A, Rush J, Fields S, Krogan L, Vilén J. Global analysis of phosphorylation and ubiquitylation cross-talk in protein degradation. Nat Methods 2013;10(7):676–82. https://doi.org/10.1038/nmeth.2519

[20] Holt L, Tuch B, Vilén J, Johnson A, Gygi S, Morgan D. Global analysis of Cdk1 substrate phosphorylation sites provides insights into evolution. Science 2009;325(5948):1682–6. https://doi.org/10.1126/science.1172867

[21] Perez-Valle J, Jenkins H, Merchan S, Montiel V, Ramos J, Sharma S, Serrano R, Yenush L. Key role for intracellular K+ and protein kinases Sat4/Hal4 and Hal5 in the plasma membrane stabilization of yeast nutrient transporters. Mol Cell Biol 2007;27(16):5725–36. https://doi.org/10.1128/MCB.01375-06

[22] Portillo F, Mulet J, Serrano R. A role for the non-phosphorylated form of yeast Snf1: tolerance to toxic cations and activation of potassium transport. FEBS Lett 2005;579(2):512–6. https://doi.org/10.1016/j.febslet.2004.12.019

[23] Casado C, Yenush L, Melero C, Ruiz C, Serrano R, Perez-Valle J, Arino J, Ramos J. Regulation of Trk-dependent potassium transport by the calcineurin pathway involves the Hal5 kinase. FEBS Lett 2010;584(11):2415–20. https://doi.org/10.1016/j.febslet.2010.04.042

[24] Yenush L, Merchan S, Holmes J, Serrano R. pH-responsive, posttranslational regulation of the Trk1 potassium transporter by the type 1-related Ppz1 phosphatase. Mol Cell Biol 2005;25(19):8683–92. https://doi.org/10.1128/MCB.25.19.8683-8692.2005

[25] Forment J, Mulet J, Vicente O, Serrano R. The yeast SR protein kinase Sky1p modulates salt tolerance, membrane potential and the Trk1,2 potassium transporter. Biochim Biophys A 2002;1565(1):36–40. https://doi.org/10.1016/s0005-2736(02)00503-5

[26] Bridges D, Moorhead G. 14-3-3 proteins: a number of functions for a numbered protein. Sci STKE 2004;296:10. https://doi.org/10.1126/stke.2962005re10

[27] Shi L, Ren A, Zhu J, Yu H, Jiang A, Zheng H, Zhao M. 14-3-3 Proteins: a window for a deeper understanding of fungal metabolism and development. World J Microbiol Biotechnol 2019;35(2):24. https://doi.org/10.1007/s11274-019-2597

[28] Smidova A, Alblova M, Kalabova D, Psenakova K, Rosulek M, Herman P, Obsil T, Obsilova V. 14-3-3 Protein masks the nuclear localization sequence of caspase-2. FEBS J 2018;285(22):4196–213. https://doi.org/10.1111/febs.14670

[29] Kalabova D, Filandr F, Alblova M, Petrvalska O, Horvath M, Man P, Obsil T, Obsilova V. 14-3-3 Protein binding blocks the dimerization interface of caspase-2. FEBS J 2020;287(16):3494–510. https://doi.org/10.1111/febs.15215

[30] van Heusden G. 14-3-3 Proteins: insights from genome-wide studies in yeast. Genomics 2009;94(5):287–93. https://doi.org/10.1016/j.ygeno.2009.07.004

[31] Bruckmann A, Steensma H, de Mattos M, van Heusden G. Regulation of transcription by Saccharomyces cerevisiae 14-3-3 Proteins. Biochem J 2004;382(3):867–75. https://doi.org/10.1042/BJ20031885

[32] Kakiuchi K, Yamauchi Y, Taoka M, Iwago M, Fujita T, Ito T, Song S, Isobe T, Ichimura T. Proteomic analysis of in vivo 14-3-3 interactions in the yeast Saccharomyces cerevisiae. Biochemistry 2007;46(26):7781–92. https://doi.org/10.1021/bi700501t

[33] van Heusden G, Steensma H. Yeast 14-3-3 proteins. Yeast 2006;23(3):159–71. https://doi.org/10.1002/yea.1338

[34] Capera J, Serrano-Novillo C, Navarro-Pérez M, Cassinelli S, Felipe A. The potassium channel odyssey: mechanisms of traffic and membrane arrangement. Int J Mol Sci 2019;20(3):734. https://doi.org/10.3390/ijms20030734

[35] Smidova A, Stankova K, Petrvalska O, Lazar J, Sychrova H, Obsil T, Zimmermannova O, Obsilova V. The Activity of Saccharomyces cerevisiae Na+, K+/H+ Antiporter Nha1 Is negatively regulated by 14-3-3 protein binding at serine 481. Biochim Biophys A 2019;1866(12):118534. https://doi.org/10.1016/j.bbamcr.2019.118534

[36] Duby G, Poreba W, Piotrowiak D, Bobik K, Derua R, Waelkens E, Boutry M. Activation of plant plasma membrane H+-ATPase by 14-3-3 proteins is negatively controlled by two phosphorylation sites within the H+-ATPase C-terminal region. J Biol Chem 2009;284(7):4213–21. https://doi.org/10.1074/jbc.M807311200

[37] Sottocornola B, Gazzarrini S, Olivari C, Romani G, Valbuzzi P, Thiel G, Moroni A. 14-3-3 proteins regulate the potassium channel KAT1 by dual modes. Plant Biol 2008;10(2):231–6. https://doi.org/10.1111/j.1438-8677.2007.00028

[38] Guldener U, Fielder T, Beinhauer J, Hegemann J. A new efficient gene disruption cassette for repeated use in budding yeast. Nucleic Acid Res 1996;24(13):2519–24. https://doi.org/10.1093/nar/24.13.2519

[39] Hanscho M, Ruckerbauer DE, Chauhan N, Hofbauer HF, Krahulec S, Nidetzky B, Kohlwein SD, Zanghellini J, Natter K. Nutritional requirements of the BY series of Saccharomyces cerevisiae strains for optimum growth. FEMS Yeast Res 2012;12(7):796–808. https://doi.org/10.1111/j.1567-1364.2012.00830

[40] Zimmermannova O, Felcmanova K, Rosas-Santiago P, Papouskova K, Pantoja O, Sychrova H. Erv14 cargo receptor participates in regulation of plasma-membrane potential, intracellular pH and potassium homeostasis via its interaction with K+-specific transporters Trk1 and Tok1. Biochim Biophys A 2019;1866(9):1376–88. https://doi.org/10.1016/j.bbamcr.2019.05.005

[41] Crooks G, Hon G, Chandonia J, Brenner S. WebLogo: a sequence logo generator. Genome Res 2004;14(6):1188–90. https://doi.org/10.1101/gr.849004

[42] Blom N, Gammeltoft S, Brunak S. Sequence and structure-based prediction of eukaryotic protein phosphorylation sites. J Mol Biol 1999;294(5):1351–62. https://doi.org/10.1006/jmbi.1999.3310

[43] Madeira F, Tinti M, Murugesan G, Berrett E, Stafford M, Toth R, Cole C, MacKintosh C, Barton G. 14-3-3-Pred: improved methods to predict 14-3-3-binding phosphopeptides. (oi). Bioinformatics 2015;31(14):2276–83. https://doi.org/10.1093/bioinformatics/btv133

[44] Jumper J, Evans R, Pritzel A, Green T, Figurnov M, Ronneberger O, Tunyasuvunakool K, Bates R, Zidek A, Potapenko A, Bridgland A, Meyer C, Kohl S, Ballard A, Cowie A, Romera-Paredes B, Nikolov S, Jain R, Adler J, Back T, Petersen S, Reiman D, Clancy E, Zielinski M, Steinegger M, Pacholska M, Berghammer T, Bodestein S, Silver D, Vinalys O, Senior A, Kavukcuoglu K, Kohli P, Hassabis D. Highly accurate protein structure prediction with AlphaFold. Nature 2021;596(7873):583–9. https://doi.org/10.1038/s41586-021-03819-2

[45] Varadi M, Anyango S, Deshpande M, Nair S, Natassia C, Yordanova G, Yuan D, Stroe O, Wood G, Laydon A, Zidek A, Green T, Tunyasuvunakool K, Petersen S, Jumper J, Clancy E, Green R, Vora A, Lutfi M, Figurnov M, Cowie A, Hobbs N, Kohli P, Kleywegt G, Birney E, Hassabis D, Velnkar S. AlphaFold protein structure database: massively expanding the structural coverage of protein-sequence space with high-accuracy models. Nucleic Acid Res 2021;50(1):439–44. https://doi.org/10.1093/nar/gkab1061

[46] Goddard T, Huang C, Meng E, Pettersen E, Couch G, Morris J, Ferrin T. UCSF chimeraX: meeting modern challenges in visualization and analysis. Protein Sci 2018;27(1):14–25. https://doi.org/10.1002/pro.3235

[47] Veisova D, Rezabkova L, Stepanek M, Novotna P, Herman P, Vecer J, Obsil T, Obsilova V. The C-terminal segment of yeast BMH Proteins exhibits different structure compared to other 14-3-3 protein isoforms. Biochemistry 2010;49(18):3853–61. https://doi.org/10.1021/bi100273k

[48] Pohl P, Joshi R, Petrvalska O, Obsil T, Obsilova V. 14-3-3-protein regulates nedd4-2 by modulating interactions between HECT and WW domains. Commun. Biol 2021;4:899. https://doi.org/10.1038/s42003-021-02419-0

[49] Miranda M, Bashi E, Vylkova S, Edgerton M, Slayman C, Rivetta A. Conservation and dispersion of sequence and function in fungal TRK potassium transporters: Focus on Candida albicans. FEMS Yeast Res 2009;9(2):278–92. https://doi.org/10.1111/j.1567-1364.2008.00471

[50] Eraso P, Mazon M, Portillo F. Yeast protein kinase Ptk2 localizes at the plasma membrane and phosphorylates in vitro the C-terminal peptide of the H+-ATPase. Biochim Biophys A 2006;1758(2):164–70. https://doi.org/10.1016/j.bbamem.2006.01.010

[51] de Nadal E, Posas F. The HOG pathway and the regulation of osmoadaptive responses in yeast. FEMS Yeast Res 2022;22(1):foac013. https://doi.org/10.1093/femsyr/foac013

[52] Taylor I, Wang Y, Seitz K, Baer J, Bennewitz S, Mooney B, Walker J. Analysis of phosphorylation of the receptor-like protein kinase HAESA during arabidopsis floral abscission. PLoS One 2016;11(1):e0147203. https://doi.org/10.1371/journal.pone.0147203

[53] White D, Unwin R, Bidels E, Pierce A, Teng H, Muter J, Greystoke B, Somerville T, Grifiths J, Lovell S, Somervaille T, Delwel R, Whetton A, Meyer S. Phosphorylation of the leukemic oncoprotein EVI1 on serine 196 modulates DNA Binding, transcriptional repression and transforming ability. PloS One 2013;8(6):e66510. https://doi.org/10.1371/journal.pone.0066510

[54] Vlastaridis P, Kyriakidou P, Chaliotis A, Van de Peer Y, Oliver S, Amoutzias G. Estimating the total number of phosphoproteins and phosphorylation sites in eukaryotic proteomes. Gigascience 2017;6(2):1–11. https://doi.org/10.1093/gigascience/giw015

[55] Davidson A. Mechanism of coupling of transport to hydrolysis in bacterial ATP-binding cassette transporters. J Bacteriol 2002;184(5):1225–33. https://doi.org/10.1128/JB.184.5.1225-1233.2002

[56] Levin E, Zhiu M. Recent progress on the structure and function of the TrkH/KtrB ion channel. Curr Opin Struct Biol 2014;27:95–101. https://doi.org/10.1016/j.sbi.2014.06.004

[57] Chen Z, Cole P. Synthetic approaches to protein phosphorylation. Curr Opin Chem Biol 2015;28:115–22. https://doi.org/10.1016/j.cbpa.2015.07.001

[58] Rezaei-Ghaleh N, Amininasab M, Kumar S, Walter J, Zweckstetter M. Phosphorylation modifies the molecular stability of β-amyloid deposits. Nat Commun 2016;7:11359. https://doi.org/10.1038/ncomms11359

[59] Yenush L, Mulet J, Arino J, Serrano R. The Ppz protein phosphatases are key regulators of K^+ and pH homeostasis: implications for salt tolerance, cell wall integrity and cell cycle progression. EMBO J 2002;21(5):920–9. https://doi.org/10.1093/emboj/21.5.920

[60] Zhao P, Zhao C, Chen D, Yun C, Li H, Bai L. Structure and activation mechanism of the hexameric plasma membrane H^+-ATPase. Nat Comm 2021;12(1). https://doi.org/10.1038/s41467-021-26782-y

[61] Camoni L, Visconti S, Aducci P, Marra M. From plant physiology to pharmacology: fusicoccin leaves the leaves. Planta 2019;249(1):49–57. https://doi.org/10.1007/s00425-018-3051-2